ELSEVIER

Nuclear Physics A 609 (1996) 147–162

NUCLEAR PHYSICS A

Strong coupled-channel effects in the ^{9}Be(^{3}He,^{3}He), ^{9}Be(^{3}He,^{7}Be) and (^{3}He,^{6}Li) reactions at $E(^{3}\mathrm{He}) = 60$ MeV

A.T. Rudchik [a], E.I. Koshchy [b], A. Budzanowski [c], R. Siudak [c], A. Szczurek [c], I. Skwirczyńska [c], Yu.G. Mashkarov [b], L. Głowacka [e], J. Turkiewicz [e], I.I. Zalyubovsky [b], V.A. Ziman [a], N.T. Burtebayev [d], A.D. Duysebayev [d], V.V. Adodin [d]

[a] *Institute for Nuclear Research, 252028 Kiev (Kyiv), Ukraine*
[b] *Kharkiv State University, 310077 Kharkiv, Ukraine*
[c] *H. Niewodniczański Institute of Nuclear Physics, PL-31-342 Cracow, Poland*
[d] *Institute of Nuclear Physics, Alma Ata, Kazakhstan*
[e] *A. Soltan Institute for Nuclear Studies, PL-00-681 Warsaw, Poland*

Received 25 March 1996; revised 31 July 1996

Abstract

The angular distributions of the ^{9}Be(^{3}He,^{7}Be)^{5}He and ^{9}Be(^{3}He,^{6}Li)^{6}Li reactions were measured at the energy of 60 MeV for the transitions to the ground states of ^{5}He and ^{6}Li and 2.185 MeV (3^{+}), 5.37 MeV (2^{+}) + 5.65 MeV (1^{+}) excited states of ^{6}Li. The experimental data were analyzed using the coupled reaction channels (CRC) model including one- and two-step cluster transfers and cluster spectroscopic amplitudes calculated in the framework of the translation-invariant shell model. It was found that the coupling with inelastic channels and reorientation process modifies the elastic scattering cross section at large angles and allows one to describe the cross section satisfactorily. The cluster transfers are unimportant. The ^{9}Be(^{3}He,α)^{8}Be reaction was included in the analysis to determine the optical potential of the intermediate α + ^{8}Be channel in two-step transfer. It was found that in the ^{9}Be(^{3}He,^{7}Be)^{5}He reaction the α-transfer dominates only at small angles while the transfer of the 2n-cluster at large angles. In the angular range $\theta_{cm} \simeq 30°$–$80°$ the cross sections are determined by the sequential transfers of the neutron and ^{3}He-cluster as well as deuteron and deuteron. The transitions to highly excited states of the intermediate ^{8}Be and ^{7}Li nuclei give large contributions to the cross sections. In the ^{9}Be(^{3}He,^{6}Li)^{6}Li reaction the t-cluster transfer dominates only for the transitions to the excited states of ^{6}Li. The cross section for the transition to the ground state of ^{6}Li is determined by the sequential transfer of the neutron and deuteron. Good agreement between measured and calculated cross sections was achieved.

PACS: 24.50.+g; 24.10.Eq; 25.45.Hi

Keywords: NUCLEAR REACTIONS ^{9}Be(^{3}He,^{7}Be), (^{3}He,^{6}Li), $E = 60$ MeV; measured $\sigma(\theta)$, coupled reaction channels model analysis.

PII S0375-9474(96)00288-6

1. Introduction

Multi-nucleon transfer reactions can be effectively used to study the nuclear structure only in the case when their mechanism is well established. In the past it was possible to calculate the absolute cross sections of these reactions mainly for the one-step processes and exclusively for the 1p-shell nuclei. Here the main theoretical problems concern the calculations of heavy-cluster spectroscopic amplitudes and the couplings between one- and multi-step reaction channels. Some progress was achieved in the calculations of heavy-cluster spectroscopic amplitudes for the 1s- and 1p-shell nuclei [1–4] and in the direct one-step reaction models [5–8]. For some reactions a surprisingly good description of experimental data by the exact-finite-range (EFR) DWBA cross sections was observed assuming transfers of heavy-clusters including unstable ^{5}He, ^{5}Li, ^{8}Be clusters (see e.g. [3,9,10]). In spite of the phenomenological success a natural question arises about reliability of this theoretical approach. The answer to this question can be obtained only by studying both one- and multi-step processes in the framework of the coupled reaction channels (CRC) model [11]. It was found only recently that two-step transfers may play an important role in the reactions with light ions [12]. This stimulated us in the present work to study in detail the couplings between one- and two-step processes in the reactions for which the cluster and nucleon spectroscopical amplitudes can be calculated.

In the present work we study one- and two-step cluster transfers in the ^{9}Be(^{3}He,α)^{8}Be, ^{9}Be(^{3}He,^{7}Be)^{5}He and ^{9}Be(^{3}He,^{6}Li)^{6}Li reactions at the energy of 60 MeV. The role of cluster transfers in the large angle ^{3}He scattering on the ^{9}Be target was also investigated here.

Due to strong binding of the alpha-clusters the two-step n + ^{3}He transfer in the ^{9}Be(^{3}He,^{7}Be)^{5}He reaction can be enhanced by a formation of an intermediate α + ^{8}Be channel which has large cross section for the transition to the high-energy excited states of ^{8}Be which was observed in the ^{9}Be(^{3}He,α)^{8}Be reaction [13]. To estimate correctly the cross section of this transfer we have determined the optical potential parameters for the intermediate ^{8}Be + α channel using experimental data of ^{9}Be(^{3}He,α)^{8}Be reaction [21].

To the best of our knowledge the angular distributions of the ^{9}Be(^{3}He,^{7}Be)^{5}He reaction were not studied before. That is the reason why we put a special attention to studying this reaction at $E(^{3}\mathrm{He})$ = 60 MeV.

The ^{9}Be(^{3}He,^{6}Li)^{6}Li reaction is convenient to investigate the sequential n+d-, d+n-, 2n+p- and α+p- transfers and to make a comparison with the t-transfer. It can be expected that the n+d-transfer which proceeds through the α + ^{8}Be intermediate channel can considerably contribute to the reaction cross section.

The ^{9}Be(^{3}He,^{6}Li)^{6}Li reaction was studied in the past at rather low energies of 6–10 MeV [14,15]. A zero-range (ZR) DWBA model was used to analyze the data assuming the t-cluster transfer mechanism. In Ref. [16] the energy spectra of ^{6}Li from the ^{9}Be(^{3}He,^{6}Li)^{6}Li reaction at 45 MeV were investigated. Preliminary data of the ^{9}Be(^{3}He,^{6}Li)^{6}Li reaction at 60 MeV were published in Ref. [17]. The data were

analyzed within the EFR DWBA model [5,6] assuming the t-cluster transfer mechanism. The description of the data was rather poor and the couplings of one- and two-step transfers were not included in the calculations.

In this article we present the data of the ^{9}Be(^{3}He,^{7}Be)^{5}He and ^{9}Be(^{3}He,^{6}Li)^{6}Li reactions at the energy $E(^{3}\mathrm{He})$ = 60 MeV and the results of the CRC analysis taking into account all possible one- and two-step transfers. The cross section of the ^{9}Be(^{3}He,^{6}Li)^{6}Li reaction presented in Ref. [17] was corrected by a factor of about 2. In the present CRC analysis we used the data of the ^{9}Be + ^{3}He scattering at $E(^{3}\mathrm{He})$ = 60 MeV from Ref. [17]. Somewhat older data for elastic ^{3}He + ^{9}Be scattering have been presented in Ref. [21].

The paper is organized as follows: in Section 2 we describe the experimental procedure, the results of the CRC analysis of the data including one- and two-step processes are discussed in Section 3. Remarks and conclusions close the paper.

2. Experimental procedure

The cross sections of the ^{9}Be(^{3}He,^{7}Be)^{5}He and ^{9}Be(^{3}He,^{6}Li)^{6}Li reactions were measured with the ^{3}He beam of the Alma Ata (Kazakhstan) cyclotron at the energy of 60 MeV [17]. The beam energy spread did not exceed 0.5%. A self-supporting $\sim$ 500 μg/cm^2 foil of ^{9}Be was used as a target . The reaction products were detected with the $\Delta E - E$ spectrometer, consisting of the $\sim$ 50 μm (ΔE) and $\sim$ 500 μm (E) silicon detectors. The electronic system was able to identify the reaction products such as ^{6}Li, ^{7}Li and ^{7}Be.

Typical energy spectra of ^{6}Li and ^{7}Be are shown in Fig. 1. As seen from the ^{6}Li spectrum (upper panel in Fig. 1), the transitions to the ground (1^+), 2.185 MeV (3^+) and 5.37 MeV ($2^+, T = 1$) + 5.65 MeV (1^+) excited states of the ^{6}Li nucleus have fairly large intensities which allowed us to analyze their angular distributions. The ^{7}Be energy spectrum (lower panel in Fig. 1) indicates a large probability for the transitions to the ground states of the ^{5}He nucleus and to the ground ($\frac{3}{2}^-$) and first excited 0.429 MeV ($\frac{1}{2}^-$) states of ^{7}Be (unresolved in the present experiment).

The angular distribution of the ^{9}Be(^{3}He,^{7}Be)^{5}He reaction was determined for the transitions to the ground and first excited states of ^{7}Be (unresolved states) in the angular range of $\theta_{\mathrm{cm}} \simeq 15°$–$110°$ (Fig. 5). The statistical errors and the errors caused by a continuum background are shown in the figure.

The angular distributions of the ^{9}Be(^{3}He,^{6}Li)^{6}Li reaction were measured for the transitions to the ground (1^+), 2.185 MeV (3^+) and 5.37 MeV ($2^+, T = 1$) + 5.65 MeV (1^+) excited states of ^{6}Li in the angular range of $\theta_{\mathrm{cm}} \simeq 15°$–$70°$. The angular distributions of the ^{9}Be(^{3}He,^{6}Li)^{6}Li reaction are shown in Figs. 6, 7 and 8. The error bars shown in the figures include both statistical errors and the errors due to the background subtraction. Because of the particle identity in the exit channel the angular distribution for the transition to the ground state of ^{6}Li is symmetric around $\theta_{\mathrm{cm}} = 90°$.

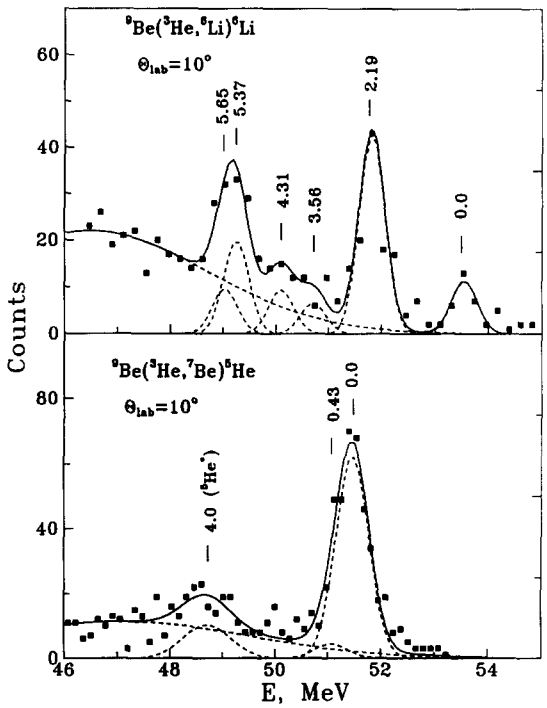

Fig. 1. The energy spectra of ^{6}Li from the ^{9}Be(^{3}He,^{6}Li)^{6}Li reaction (upper panel) and ^{7}Be from the ^{9}Be(^{3}He,^{7}Be)^{5}He reaction (lower panel) at the energy $E(^3\text{He}) = 60$ MeV for $\theta_{lab} = 12°$.

The reaction cross sections were normalized to the ^{3}He elastic scattering, which was measured simultaneously with reactions mentioned above. Therefore, the normalization error of the reaction cross section is the same as for elastic scattering and is about 15%.

3. Analysis of the data

3.1. The ^{9}Be + ^{3}He elastic scattering

In order to describe different reaction channels in the framework of CRC model a special attention must be paid to the elastic scattering, because the CRC cross sections depend strongly on the optical model (OM) potentials. The parameters of the OM potential of the ^{9}Be + ^{3}He elastic scattering at energy $E(^3\text{He}) = 60$ MeV were obtained by fitting to the data from Ref. [17] using a code SPI-GENOA [20]. We restricted the fitting procedure only to forward angles ($\theta_{cm} < 120°$), where the contribution of other processes is expected to be negligible. The angular distribution of the ^{9}Be + ^{3}He elastic scattering at $E(^3\text{He}) = 60$ MeV is shown in Fig. 2 and two sets (A,B) of the Woods–Saxon potential parameters fitted to the elastic scattering data are listed in Table 1. In the upper panel we show absolute cross sections and in the lower panel

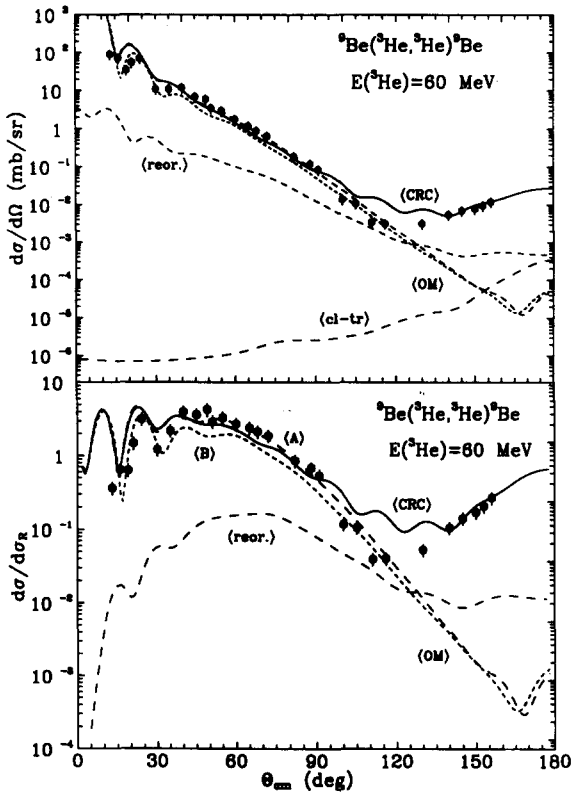

Fig. 2. The angular distribution of the ^{9}Be + ^{3}He elastic scattering at the energy $E(^3\text{He})$ = 60 MeV. The shown curves are: the CRC cross section (solid curves ⟨CRC⟩), the OM cross section (dashed ⟨OM⟩ for potentials A and B (Table 1)), the cross section of reorientation process (dashed ⟨reor.⟩) and the cross section of cluster transfers (dashed ⟨cl-tr⟩) for which corresponding diagrams are given in Fig. 3(I). The lower panel presents the elastic cross section divided by Rutherford cross section.

Table 1
Parameters of the Woods–Saxon optical model potentials

T + P	V (MeV)	r_V (fm)	a_V (fm)	W_S (MeV)	r_W fm)	a_W (fm)	r_c (fm)	Ref. or name
^{9}Be+^{3}He	143.4	0.605	1.100	38.28 (35.5 [a])	0.833	1.170	0.738	A
	143.4	0.560	1.000	36.40	0.804	1.170	0.738	B
^{6}Li+^{6}Li	122.5	0.577	0.905	51.71	0.540	1.178	0.588	[18]
^{7}Li+^{5}Li	122.5	0.577	0.610	51.71	0.540	1.178	0.588	
^{7}Be+^{5}He	122.5	0.577	0.610	51.71	0.540	1.178	0.588	
^{8}Be+^{4}He	143.4	0.605	1.350	38.28	1.500	1.670	0.738	C
	121.0	0.656	0.770	22.40	0.927	0.500	0.720	D
^{10}B+d	84.7	0.700	0.609	5.29 [b]	0.864	1.003	0.820	[23]

[a] used in CRC calculation;

[b] W_D (derivative of the Woods–Saxon shape); $R_i = r_i(A_T^{1/3} + A_P^{1/3})$, $i = V, W$.

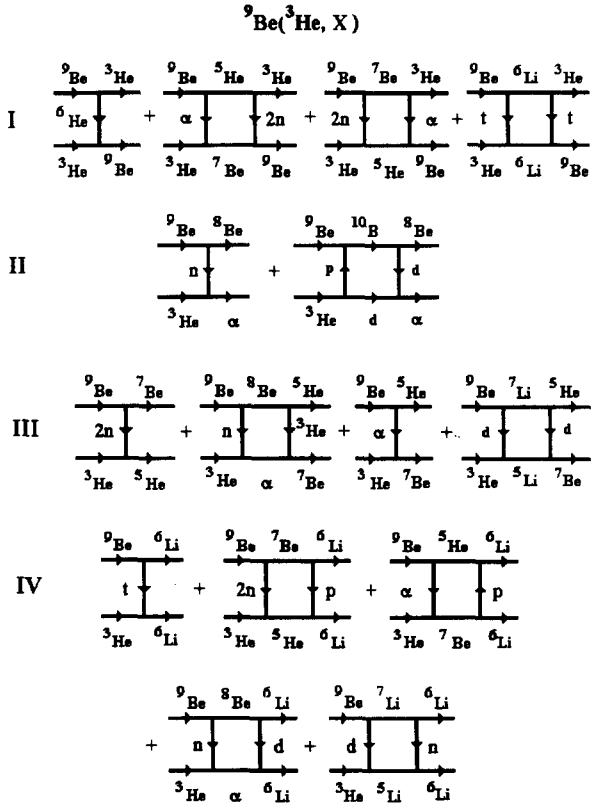

Fig. 3. The diagrams of the one- and two-step transfer reactions included in the CRC analysis. The diagrams for the ^{9}Be(^{3}He,^{9}Be)^{3}He reaction are marked as I, for ^{9}Be(^{3}He,α)^{8}Be as II, for ^{9}Be(^{3}He,^{7}Be)^{5}He as III and for ^{9}Be(^{3}He,^{6}Li)^{6}Li reaction as IV.

the cross sections normalized to the Rutherford cross section. Potential A describes satisfactorily the experimental data up to 120°. In the region 15–30° it reproduces the main structure of the angular distribution but misses somewhat the depth of the fluctuations. On the contrary, potential B describes satisfactorily only the latter region but fails in the remaining region. Since the χ^2 value for potential A is considerably smaller than for potential B, in the following we shall present only results obtained with potential A.

In the CRC analysis we have used a code FRESCO [11]. The reverse direction couplings were taken into account in the CRC calculations. Both inelastic scattering and reorientation were included in the CRC analysis. Since the cross sections to inelastic scattering channels were not determined in the present experiment we have taken into account a corresponding deformation parameter for the ground state of ^{9}Be from Ref. [22] ($\beta_2 = 0.5$) and used a deformation length $\delta_2 = 0.85$ fm (($\beta_2 = 0.63$) which gave a good description of the experimental data. The quadrupole transitions to the 2.429 MeV ($\frac{5}{2}^-$) and 6.8 MeV ($\frac{7}{2}^-$) excited states of ^{9}Be were included in the coupling scheme.

We have assumed that these states are of rotational nature. The reaction channels for the one- and two-step transfers shown in Fig. 3 were included in the coupling scheme.

The parameters of the Woods–Saxon potentials used in the CRC calculations are given in Table 1. The OM potential of ^{7}Li + ^{6}Li elastic scattering at the energy 78 MeV [18] was used for the ^{6}Li + ^{6}Li channel. The Woods–Saxon potential parameters for the ^{8}Be + α and ^{7}Be + ^{5}He channels were obtained from the analysis of the ^{9}Be(^{3}He,α)^{8}Be [13] and ^{9}Be(^{3}He,^{7}Be)^{5}He reaction data. According to the charge symmetry of nuclear interaction we used the same OM potential for the ^{7}Li + ^{5}Li and ^{7}Be + ^{5}He channels.

The prior interaction was taken for the first step of sequential transfers and one-step processes. The second step was calculated with the post interaction. The cluster and nucleon spectroscopic amplitudes (SA) used in the CRC calculations are listed in Table 2. These SA were calculated in the translation-invariant shell model (TISM) [1], with the help of a code DESNA [2,3]. The 2n-transfer was approximated by the transfer of the neutron pair with spin 0. In the SA-calculations we used the shell-model wave functions tabulated by Boyarkina [19].

The cluster bound-state wave functions were calculated with the standard procedure by fitting the depth of a Woods–Saxon potential to obtain the cluster binding energy. The geometric parameters of the bound-state potentials were fixed at $a = 0.65$ fm and $r_0 = \bar{r}_0 A^{1/3}/(A_c^{1/3} + A_x^{1/3})$ fm, where A, A_c and A_x are the masses of a composite system, core and cluster, respectively. We have found that varying the parameter $\bar{r}_0$ in the range of 1.0–1.4 fm does not lead to significantly different results. Therefore, in the final calculation we have fixed $\bar{r}_0 = 1.25$ fm known to be a universal parameter for light nuclei.

The calculated cross sections of the ^{9}Be + ^{3}He elastic scattering are shown in Fig. 2. In order to understand the nature of the backward angle enhancement of the angular distribution we have calculated the contributions of one- (^{6}He) and two-step (α+2n, 2n+α, t+t) transfer processes shown diagrammatically in Fig. 3. As seen from the upper panel of Fig. 2 these processes (dashed curve marked with ⟨cl-tr⟩) give only a small contribution to backward angle elastic scattering and cannot explain the experimentally observed enhancement. A much larger contribution in this region is obtained from a reorientation process (dashed line marked by ⟨reor.⟩) which is however insufficient to explain experimental data. An interesting conclusion can be drawn by a comparison of the CRC (solid) and OM (dashed) angular distributions. We find that the coupling between the channels significantly modifies the elastic channel cross section at large angles, where a pick-up of heavy cluster plays usually a dominant role. In our case the CRC cross sections agree well with the ^{9}Be + ^{3}He elastic scattering data in the whole angular range.

Table 2
Cluster spectroscopic amplitudes S_x for the $A = C + x$ systems

A	C	x	nlj	S_x
^{3}He	d	p	$1S_{1/2}$	1.225
α	d	d	$1S_1$	1.732
α	^{3}He	n	$1S_{1/2}$	−1.414
^{5}He	^{3}He	2n	$1P_1$	−0.913
^{5}Li	^{3}He	d	$1P_1$	0.456
			$1P_2$	1.021
^{6}Li	^{3}He	t	$2S_{1/2}$	−0.943
^{6}Li	α	d	$2S_1$	1.061
^{6}Li	^{5}He	p	$1P_{1/2}$	−0.596
			$1P_{3/2}$	0.667
^{6}Li	^{5}Li	n	$1P_{1/2}$	0.596
			$1P_{3/2}$	−0.667
^{6}Li$^{*}_{2.19}$	^{3}He	t	$1D_{5/2}$	−0.943
^{6}Li$^{*}_{2.19}$	α	d	$1D_3$	1.061
^{6}Li$^{*}_{2.19}$	^{5}He	p	$1P_{3/2}$	−1.095
^{6}Li$^{*}_{2.19}$	^{5}Li	n	$1P_{3/2}$	1.095
^{6}Li$^{*}_{5.37}$	^{3}He	t	$1D_{3/2}$	−0.596
			$1D_{5/2}$	−0.730
^{6}Li$^{*}_{5.37}$	^{5}He	p	$1P_{1/2}$	−0.632
			$1P_{3/2}$	−0.632
^{6}Li$^{*}_{5.37}$	^{5}Li	n	$1P_{1/2}$	−0.632
			$1P_{3/2}$	−0.632
^{6}Li$^{*}_{5.65}$	^{3}He	t	$1D_{3/2}$	0.943
^{6}Li$^{*}_{5.65}$	α	d	$1D_1$	1.061
^{6}Li$^{*}_{5.65}$	^{5}He	p	$1P_{1/2}$	0.333
			$1P_{3/2}$	0.298
^{6}Li$^{*}_{5.65}$	^{5}Li	n	$1P_{1/2}$	−0.333
			$1P_{3/2}$	−0.298
^{7}Li	^{5}He	d	$2S_1$	−0.674
			$1D_1$	−0.121
			$1D_3$	0.676
^{7}Li	^{6}Li	n	$1P_{1/2}$	−0.657
			$1P_{3/2}$	−0.735
^{7}Li	^{6}Li$^{*}_{2.19}$	n	$1P_{3/2}$	0.738
^{7}Li	^{6}Li$^{*}_{5.37}$	n	$1P_{1/2}$	−0.360
			$1P_{3/2}$	0.360
^{7}Li	^{6}Li$^{*}_{5.65}$	n	$1P_{1/2}$	0.147
			$1P_{3/2}$	−0.132
^{7}Li$^{*}_{0.478}$	^{5}He	d	$2S_1$	−0.852
			$1D_1$	0.191
			$1D_2$	0.572
^{7}Li$^{*}_{0.478}$	^{6}Li	n	$1P_{1/2}$	0.329
			$1P_{3/2}$	0.930
^{7}Li$^{*}_{0.478}$	^{6}Li$^{*}_{5.65}$	n	$1P_{1/2}$	0.588
			$1P_{3/2}$	−0.208
^{7}Li$^{*}_{4.63}$	^{5}He	d	$1D_2$	−0.572
			$1D_3$	−0.700
^{7}Be	^{3}He	α	$2P_1$	1.091
^{7}Be	α	^{3}He	$2P_{3/2}$	−1.091

Table 2 — continued

A	C	x	nlj	S_x
^{7}Be	^{5}Li	d	$2S_1$	−0.674
			$1D_1$	−0.121
			$1D_3$	0.676
^{7}Be	^{6}Li	p	$1P_{1/2}$	−0.657
			$1P_{3/2}$	−0.735
^{7}Be	^{6}Li$^{*}_{2.19}$	p	$1P_{3/2}$	0.738
^{7}Be	^{6}Li$^{*}_{5.37}$	p	$1P_{1/2}$	0.360
			$1P_{3/2}$	0.360
^{7}Be	^{6}Li$^{*}_{5.65}$	p	$1P_{1/2}$	0.147
			$1P_{3/2}$	−0.132
^{7}Be$^{*}_{0.43}$	^{3}He	α	$2P_1$	−1.091
^{7}Be$^{*}_{0.43}$	α	^{3}He	$2P_{1/2}$	1.091
^{8}Be	^{5}He	^{3}He	$2P_{3/2}$	−1.102
^{7}Be$^{*}_{0.429}$	^{5}Li	d	$2S_1$	−0.852
			$1D_1$	0.191
			$1D_2$	0.572
^{8}Be	^{6}Li	d	$2S_1$	1.217
^{8}Be	^{6}Li$^{*}_{2.19}$	d	$1D_3$	0.744
^{8}Be	^{6}Li$^{*}_{5.65}$	d	$1D_1$	0.487
^{8}Be$^{*}_{2.94}$	^{5}He	^{3}He	$2P_{1/2}$	0.652
			$2P_{3/2}$	0.652
			$1F_{5/2}$	−0.228
			$1F_{7/2}$	−0.558
^{8}Be$^{*}_{16.63}$	^{5}He	^{3}He	$2P_{1/2}$	−0.302
			$1F_{5/2}$	−0.411
			$1F_{7/2}$	0.402
^{8}Be$^{*}_{16.97}$	^{5}He	^{3}He	$2P_{1/2}$	−0.302
			$1F_{5/2}$	−0.411
			$1F_{7/2}$	0.402
^{8}Be$^{*}_{17.6}$	^{5}He	^{3}He	$2P_{1/2}$	−0.130
			$2P_{3/2}$	−0.116
			$1F_{5/2}$	−0.652
^{8}Be$^{*}_{19.22}$	^{5}He	^{3}He	$2P_{3/2}$	−0.427
			$1F_{5/2}$	0.124
			$1F_{7/2}$	−0.416
^{9}Be	^{3}He	^{6}He	$2P_1$	0.236
^{9}Be	^{5}He	α	$3S_0$	−0.810
			$2D_2$	−0.536
^{9}Be	^{6}Li	t	$2P_{1/2}$	−0.192
			$2P_{3/2}$	−0.215
^{9}Be	^{6}Li$^{*}_{2.19}$	t	$2P_{3/2}$	−0.594
			$1F_{5/2}$	−0.094
			$1F_{7/2}$	−0.316
^{9}Be	^{6}Li$^{*}_{5.37}$	t	$2P_{1/2}$	−0.290
			$2P_{3/2}$	0.290
			$1F_{5/2}$	−0.129
			$1F_{7/2}$	0.316
^{9}Be	^{6}Li$^{*}_{5.65}$	t	$2P_{1/2}$	−0.118
			$2P_{3/2}$	0.106
			$1F_{5/2}$	−0.324

Table 2 — continued

A	C	x	nlj	S_x
^{9}Be	^{7}Li	d	$2S_1$	−0.226
			$1D_1$	0.111
			$1D_3$	−0.624
^{9}Be	^{7}Li$^{*}_{0.478}$	d	$2S_1$	0.202
			$1D_1$	0.124
			$1D_2$	−0.373
^{9}Be	^{7}Li$^{*}_{4.63}$	d	$1D_2$	0.271
			$1D_3$	−0.332
^{9}Be	^{7}Be	2n	$2S_0$	0.247
			$1D_2$	0.430
^{9}Be	^{7}Be$^{*}_{0.43}$	2n	$1D_2$	0.430
^{9}Be	^{8}Be	n	$1P_{3/2}$	0.866
^{9}Be	^{8}Be$^{*}_{2.94}$	n	$1P_{1/2}$	−0.573
			$1P_{3/2}$	0.573
^{9}Be	^{8}Be$^{*}_{16.63}$	n	$1P_{1/2}$	0.265
^{9}Be	^{8}Be$^{*}_{16.91}$	n	$1P_{1/2}$	0.265
^{9}Be	^{8}Be$^{*}_{17.63}$	n	$1P_{1/2}$	0.088
			$1P_{3/2}$	−0.079
^{9}Be	^{8}Be$^{*}_{19.22}$	n	$1P_{3/2}$	0.444
^{10}B	^{8}Be	d	$1D_3$	0.811
^{10}B	^{9}Be	p	$1P_{3/2}$	1.185

3.2. The $^{9}Be(^{3}He,\alpha)^{8}Be$ reaction

Because the ^{9}Be(^{3}He,α)^{8}Be reaction constitutes the intermediate channel for processes discussed in the further part of the paper, we have included it in the CRC analysis. The cross section for this reaction depends on the potential for the α + ^{8}Be channel which cannot be obtained in the standard manner from elastic scattering. In order to determine the parameters of the OM potential for the α + ^{8}Be scattering, we have taken experimental data of the ^{9}Be(^{3}He,α)^{8}Be reaction at E(^{3}He) = 60 MeV from Ref. [21]. It was a practice in the past to use for the α + ^{8}Be scattering a potential from the α+^{12}C scattering, with the rescaling potential radius in an appropriate way. We applied this procedure to the ^{9}Be(^{3}He,α)^{8}Be reaction, using in the exit channel the OM potential obtained from α elastic scattering on the ^{12}C target at 90 MeV [24] (set D in Table 1). It turned out that in our case this procedure leads to cross sections by a factor 50–100 larger than experimental data. This shows that the α+^{8}Be potential must be different than that obtained from the simple procedure described above. Therefore, in the present analysis we have taken phenomenological attitude and apply the following procedure. As a starting potential we have used the potential for the entrance ^{9}Be+^{3}He channel. This leads to a result considerably better than that obtained above. To improve the fit further, we allow for modifications of the diffuseness of the real part and parameters of the imaginary potential. A good description of the data was obtained by increasing diffuseness and the radius of the imaginary part (see Table 1).

In the analysis describe above we have included n- and (p+d)-transfers (see Fig. 3).

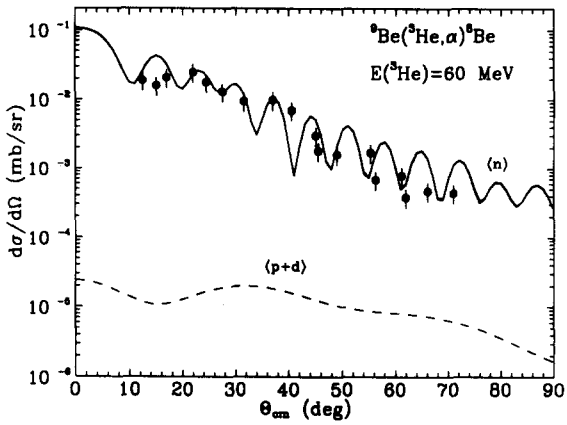

Fig. 4. The angular distribution of the ^{9}Be(^{3}He,α)^{8}Be reaction for the transition to the ground state. The experimental data (points) are taken from Ref. [21]. The solid curve represents the coherent sum of processes shown in Fig. 3. The contributions of the individual processes are shown by the ⟨n⟩ and ⟨p+d⟩ curves.

The final result is shown in Fig. 4. As was expected, the n-transfer is a dominant contribution.

3.3. The $^9Be(^3He,^7Be)^5He$ reaction

The angular distribution of the ^{9}Be(^{3}He,^{7}Be)^{5}He reaction for the transitions to the ground ($\frac{3}{2}^-$) and 0.429 MeV ($\frac{1}{2}^-$) excited states of the ^{7}Be (unresolved in the experiment) is shown in Fig. 5. The 2n-, α-cluster one-step transfers and n + ^{3}He as well as d + d two-step sequential transfers (shown at Fig. 3 (III)) were included in the couplings with the elastic and inelastic scattering channels. The CRC calculations were performed separately for the transitions to the ground ($\frac{3}{2}^-$) and 0.429 MeV ($\frac{1}{2}^-$) excited states of ^{7}Be. In each case a coherent sum of the three mechanisms given in Fig. 3 was calculated. The resulting cross sections for these transitions are shown in Fig. 5 and marked by Σ_{gs} and $\Sigma_{0.43}$, respectively.

The contributions of individual transfers for the transition to the ground state of ^{7}Be are shown in the lower panel of Fig. 5. The same experimental data as in the upper panel are shown for reference. The 2n-cluster transfer (marked by ⟨2n⟩ in Fig. 5) gives a dominant contribution to the reaction cross section at angles $\theta_{cm} > 90°$. The α-transfer (curve ⟨α⟩ in Fig. 5) plays an important role only at $\theta_{cm} < 30°$. The sequential n + ^{3}He and d + d two-step transfers (curves $\Sigma_{\langle n+^3He\rangle}$ and ⟨d+d⟩ in the lower panel of Fig. 5) are dominant in the angular range of $30° < \theta_{cm} < 80°$. One can see from Fig. 5 that only the sequential n+^{3}He and d + d transfers provide a correct slope of the CRC angular distribution in this angular range. These transfers give only a small contribution to the cross sections for the transition via the ground state of the intermediate ^{8}Be nucleus. In order to describe satisfactorily the data in this angular range we had to account for the transitions via the excited states of ^{8}Be such as 2.94 MeV (2^+), 16.627 MeV (2^+),

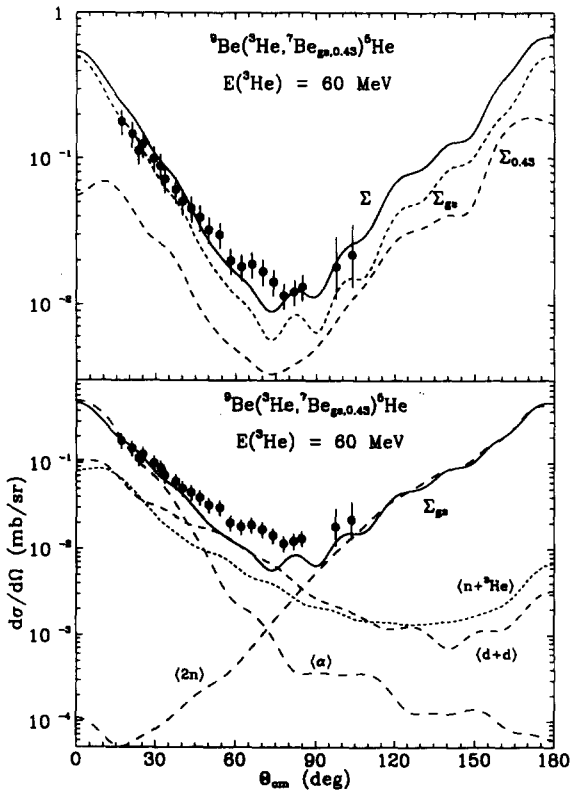

Fig. 5. The angular distribution of the ^{9}Be(^{3}He,^{7}Be$_{gs,0.429}$)^{5}He reaction for the transitions to the ground ($\frac{3}{2}^-$) and 0.429 MeV ($\frac{1}{2}^-$) excited state of ^{7}Be. The experimental data (points) are the sum of cross sections for the both transitions. In the upper panel the dashed curves show the coherent sums of cross sections for the transitions to ground (Σ_{gs}) and first excited ($\Sigma_{0.43}$) states of ^{7}Be. The Σ curve represents incoherent sum of both contributions. In the lower panel the contributions of individual mechanisms for the transition to the ground state of ^{7}Be are presented.

16.911 MeV (2^+), 19.06 MeV (3^+) and 19.22 MeV (3^+) and via the excited states of ^{7}Li such as 0.478 MeV ($\frac{1}{2}^-$), 4.63 MeV ($\frac{7}{2}^-$), 6.68 MeV ($\frac{5}{2}^-$) and 7.47 MeV ($\frac{5}{2}^-$). The resulting cross sections of the n + ^{3}He and d + d transfers for all transitions are shown in the lower panel of Fig. 5 and marked by ⟨n+^{3}He⟩ and ⟨d+d⟩. The resulting CRC cross sections including all transfers for the transition to the ground state of ^{7}Be (solid curve in the lower panel of Fig. 5, marked by Σ_{gs}) correctly describes the shape of the experimental angular distribution.

As can be seen from the upper panel of Fig. 5, the ^{9}Be(^{3}He,^{7}Be$^*_{0.43}$)^{5}He reaction gives a rather small contribution in the forward hemisphere ($\theta_{cm} < 90°$, curve $\Sigma_{0.43}$). The incoherent sum of the CRC cross sections for the transitions to the ground and 0.429 MeV excited states of ^{8}Be is shown in the upper panel of Fig. 5 (curve Σ). One can see a good agreement between CRC cross section and the experimental data.

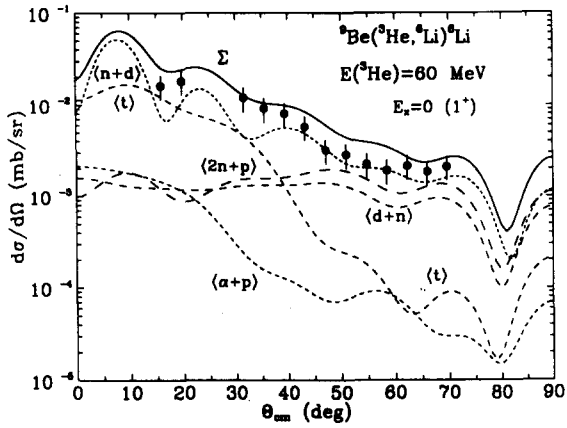

Fig. 6. The angular distribution of the ^{9}Be(^{3}He,^{6}Li)^{6}Li reaction for the transition to the ground state of the ^{6}Li nucleus. The dashed lines with the names in brackets ⟨...⟩ correspond to different individual terms. The solid line shows the coherent sum of the individual contributions.

3.4. *The ^{9}Be(^{3}He,^{6}Li)^{6}Li reaction*

The angular distribution of the ^{9}Be(^{3}He,^{6}Li$_{gs}$)^{6}Li$_{gs}$ reaction for the transition to the ground (1$^+$) state of ^{6}Li is shown in Fig. 6. The contributions of individual terms of Fig. 3 (IV) are shown in Fig. 6 by dashed curves marked by a ⟨name⟩. A first remarkable observation coming from Fig. 6 is that the sequential n + d transfer is dominant in this reaction (short-dashed line, ⟨nd⟩). The t-cluster transfer contributes to the cross section only at small angles $\theta_{cm} < 30°$ (long-dashed line, ⟨t⟩). The sequential 2n + p and d + n transfers contribute to the cross sections only at angles $\theta_{cm} > 50°$ (dashed lines, ⟨2n + p⟩ and ⟨d + n⟩, respectively). In contrast to naive expectations the sequential α + p transfer plays a rather marginal role in this reaction. The resulting CRC cross section (solid line, Σ) is in a good agreement with the experimental data. Summarizing, we have found a unique case where a two-step process dominates over the one-step mechanism in the whole angular range.

The angular distribution of the ^{9}Be(^{3}He,^{6}Li$_{gs}$)^{6}Li$_{2.185}$ reaction is shown in Fig. 7. The contributions of individual transfers (see Fig. 3 (IV)) and the resulting cross sections are shown by the dashed and solid curves, respectively. A careful comparison of Fig. 6 and 7 shows a surprisingly different structure of the contributions for the transition to the ground and first excited state of ^{6}Li. In the latter case the t-transfer plays a dominant role and the two-step processes give only small contributions at $\theta_{cm} < 60°$ and become important only at large angles.

The angular distribution of the ^{9}Be(^{3}He,^{6}Li$_{gs}$)^{6}Li$^*_{5.37+5.65}$ reaction for the transitions to the ground and 5.37 MeV (2$^+$,T = 1) + 5.65 MeV (1$^+$) (unresolved in the experiment) excited states of ^{6}Li is shown in Fig. 8 (solid curve, Σ). The CRC calculations were performed separately for the ^{9}Be(^{3}He,^{6}Li$_{gs}$)^{6}Li$^*_{5.37}$ and ^{9}Be(^{3}He,^{6}Li$_{gs}$)^{6}Li$^*_{5.65}$ reactions (dashed curves, $\Sigma_{5.37}$ and $\Sigma_{5.65}$, respectively) and then the incoherent sum (solid curve,

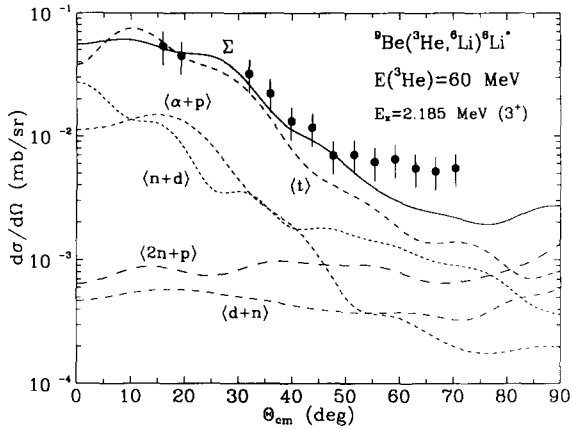

Fig. 7. The angular distribution of the ^{9}Be(^{3}He,^{6}Li)^{6}Li reaction for the transition to the 2.185 MeV (3^+) state of the ^{6}Li nucleus. For the description of lines see Fig. 6.

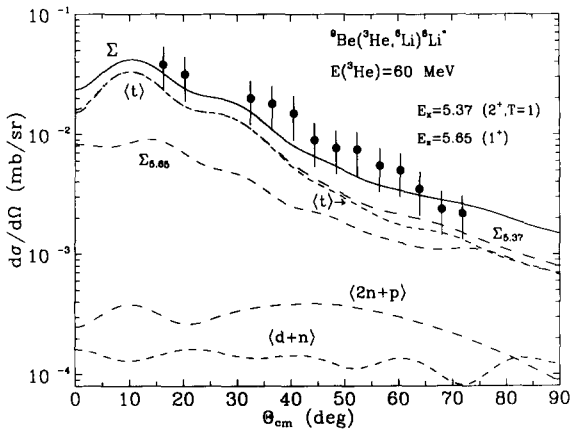

Fig. 8. The angular distribution of the ^{9}Be(^{3}He,^{6}Li)^{6}Li reaction for the transitions to the 5.37 MeV (2^+) + 5.65 MeV (1^+) states of the ^{6}Li nucleus. The lines $\Sigma_{5.37}$ and $\Sigma_{5.65}$ show the corresponding individual contributions and the solid line (Σ) is a sum of the both contributions. For the description of other lines see Fig. 6.

Σ) of the cross sections for these reactions was obtained. In Fig. 8 we show only the individual terms for the transition to the 5.37 MeV excited state of ^{6}Li (similar pattern has been obtained for the transition to the 5.65 MeV excited state of ^{6}Li) . It is obvious from Fig. 8 that the t-cluster transfer (short-dashed line, ⟨t⟩) is the dominant mechanism. The contribution of the two-step processes is almost negligible here. The transition to the 5.37 MeV excited state of ^{6}Li is dominant at angles $\theta_{cm} < 70°$. The resulting CRC cross section (solid curve, Σ) describes satisfactorily the experimental data.

4. Summary

The angular distribution of the ^{9}Be(^{3}He,^{7}Be$_{gs+0.43}$)^{5}He reaction was measured at the energy of $E(^{3}\mathrm{He})$ = 60 MeV for the transitions to the ground ($\frac{3}{2}^{-}$) and 0.429 MeV ($\frac{1}{2}^{-}$) states of ^{7}B (unresolved in the experiment) and to the ground state of ^{5}He in the angular range of $\theta_{cm} \simeq 15°$–$110°$. Simultaneously, we have determined the angular distribution of the ^{9}Be(^{3}He,^{6}Li)^{6}Li reaction in the angular region $\theta_{cm} \simeq 15°$–$70°$ for the transitions to the ground (1^{+}), 2.185 MeV (3^{+}) and 5.37 MeV (2^{+}) + 5.65 MeV (1^{+}) (unresolved in the experiment).

The experimental data were analyzed within the coupled reaction channels model (CRC) including one- and two-step transfers. Both the elastic and inelastic scattering and the one- and two-step processes were taken into account in the coupling scheme. The ^{9}Be + ^{3}He elastic scattering data of Ref. [17] at 60 MeV were used to obtain the optical potential for the entrance reaction channel. The nucleon and cluster spectroscopic amplitudes used in the CRC calculations were obtained within the translation-invariant shell model [1].

The analysis of the ^{9}Be(^{3}He,α)^{8}Be reaction at $E(^{3}\mathrm{He})$ = 60 MeV was performed to obtain an OM potential for the α + ^{8}Be channel. This potential was found starting from potential of ^{3}He + ^{9}Be channel and varying the a_V and a_W diffusenesses as well as radius of the imaginary part.

It was found that the transition to the ground state of ^{7}Be gives a dominant contribution to the ^{9}Be(^{3}He,^{7}Be$_{gs+0.43}$)^{5}He reaction data at angles $\theta_{cm} < 90°$. The α- and 2n-cluster transfers are dominant in the angular intervals $\theta_{cm} \simeq 0°$–$20°$ and $90°$–$180°$, respectively. The sequential n + ^{3}He and d + d transfers play an important role at the $\theta_{cm} \simeq 40°$–$70°$ angular range. The transitions to the excited states of the intermediate ^{8}Be and ^{7}Li nuclei give large contributions to the cross section. A good description of the experimental data was obtained within CRC model.

Both one- and two-step transfers were studied in the ^{9}Be(^{3}He,^{6}Li)^{6}Li reaction for the transitions to the ground (1^{+}) and 2.185 MeV (3^{+}), 5.37 MeV (2^{+}), 5.65 MeV (1^{+}) excited states of ^{6}Li. It was found that the sequential n + d transfer is dominant for the transition to the ground state of ^{6}Li in contrast to the transitions to the excited states where the t-transfer dominates. A good description of the experimental data was obtained within the CRC for all transitions.

The CRC analysis of the ^{9}Be(^{3}He,^{7}Be)^{5}He and ^{9}Be(^{3}He,^{6}Li)^{6}Li reactions indicates that two-step processes can play much more important role than it is commonly expected.

Acknowledgements

This work was supported in part by the Ukrainian State Committee of Science and Technology and the Polish State Committee for Scientific Research.

References

[1] Yu.F. Smirnov and Yu.M. Tchuvil'sky, Phys. Rev. C 15 (1977) 84.
[2] A.T. Rudchik and Yu.M. Tchuvil'sky, Code DESNA, Kiev Institute for Nuclear Research report KIYaI-82-12 (1982).
[3] A.T. Rudchik and Yu.M. Tchuvil'sky, Ukr. Phys. J. 30 (1985) 819;
O.F. Nemets, V.G. Neudachin, A.T. Rudchik, Yu.F. Smirnov and Yu.M. Tchuvil'sky, Nuclear associations in atomic nuclei and multi-nucleon transfer reactions (Naukova Dumka, Kiev, 1988) [in Russian].
[4] Y. Kudo et al., Prog. Theor. Phys. 59 (1978) 101;
D. Chlebowska et al., J. Phys. G 7 (1981);
E. Kwaśniewicz, M. Siemaszko, A. Szczurek and L. Jarczyk, Acta Phys. Pol. B 15 (1984) 873;
E. Kwaśniewicz et al., Acta Phys. Pol. B 16 (1985) 947;
E. Kwaśniewicz and L. Jarczyk, Nucl. Phys. A 441 (1985) 77.
[5] N. Austern, R.M. Drisko, E.C. Halbert and G.R. Satchler, Phys. Rev. B 133 (1964) 3.
[6] R.M. DeVries, Phys. Rev. C 8 (1973) 951.
[7] T. Tamura, Comput. Phys. Commun. 14 (1974) 349.
[8] P.D. Kunz, DWUCK5, University of Colorado, 1980, unpublished.
[9] L. Głowacka et al., Nucl. Phys. A 534 (1991) 349.
[10] A.T. Rudchik, in: Proc. Int. Conf. on Nuclear and Atomic Clusters, Turku, Finland, 1991, Eds. M. Brenner, T. Lönnroth and F.B. Malik (Springer, Berlin, 1992) p. 551.
[11] I.J. Thompson, Comp. Phys. Rep. 7 (1988) 167.
[12] A.T. Rudchik et al., Nucl. Phys. A 602 (1996) 211.
[13] K.P. Artemov et al., Yad. Fiz. (J. Nucl. Phys.) 7 (1968) 500.
[14] F.C. Young and A.R. Knudson, Nucl. Phys. A 184 (1972) 563.
[15] M.C. Taylor and G.C. Phillips, Nucl. Phys. A 126 (1969) 615.
[16] Th. Delbar, Gh. Grégoire, P. Belery and G. Paić, Phys. Rev. C 27 (1983) 1876.
[17] Yu.G. Mashkarov, E.I. Koshchy, I.I. Zalyubovsky, N.T. Burtebayev, A.D. Duysebayev, V.V. Adodin and A.T. Rudchik, Izv. Akad. Nauk. (Ser. Fiz.) 57 (5) (1993) 137.
[18] Yu.A. Glukhov, O.Yu. Goryunov, E.I. Koshchy, Yu.G. Mashkarov, A.T. Rudchik and S.B. Sakuta, Sov. J. Nucl. Phys. (Yad. Fiz.) 49 (1989) 774.
[19] A.N. Boyarkina, Structure of 1p-shell nuclei (Moscow State University, Moscow, 1973).
[20] B.S. Nilson, SPI-GENOA: an optical model search code, Niels Bohr Institute report (1976).
[21] V.V. Adodin et al., Yad. Fiz. (J. Nucl. Phys.) 55 (1992) 577.
[22] N. Willis et al., Nucl. Phys. A 261 (1976) 45.
[23] M. Gaillard et al., Nucl. Phys. A 119 (1968) 161.
[24] A.T. Rudchik et al., to be published.